Proceeding of the 2nd
RSI/ISM International Conference on Robotics and Mechatronics
October 15-17, 2014, Tehran, Iran

Design of an Economical SCARA Robot for Industrial Applications

Morteza Shariatee, Alireza Akbarzadeh, Ali Mousavi, and Salman Alimardani
Center of Excellence on Soft Computing and Intelligent Information Processing, Mechanical Engineering Department
Ferdowsi University of Mashhad
Mashhad, Iran
morteza_shariatee_sc@yahoo.com, ali_akbarzadeh_t@yahoo.com, ali_musavi68@yahoo.com, alimardani_salman@yahoo.com

***Abstract*— This paper presents mechanical design process of an industrial and economical SCARA robot, called FUM SCARA, designed by a team of students at the Ferdowsi University of Mashhad, in Iran. SCARA robots are among the most widely used robots in industry due to their inherent rigidity and high accuracy. The design process included, joint design, link design, controller design as well as selection of mechanical and electrical components. The challenge was to use readily available components in Iran with an eye on keeping the costs down. The FUM SCARA robot offers impressive performance such as ~±0.01 mm repeatability, maximum linear velocity of 8.5 m/s in xy plane, 0.5 seconds pick and place cycle time and a flexible control system. These specifications are in line with existing industrial robots. However, unlike the existing commercial robots, the control architecture in FUM SCARA is designed to allow for simple implementation of new control algorithms. Finally, using a PID controller, a critical trajectory in robot's workspace is traced. Results indicate low error during the fast trajectory.**

Keywords—SCARA; industrial robot; robot's mechanical design; joint design; critical trajectory

I. INTRODUCTION

Robotic manipulators with various shapes and types have become an undeniable part of industry, due to their wide range of application. Among them, SCARA robots with 3 revolute and one prismatic DOF have become popular in packaging and assembly lines. This type of robot was first introduced by Hiroshi Makino in 1979 [1],[2]. Nowadays commercial SCARA robots are made in various sizes, linear speeds and payload. Control systems of such robots are designed for common industrial applications and in general are not suitable for high level research purposes [3].

Relatively speaking, there exists a few studies on robots designs. In reference [4], authors illustrated a new non-linear direct power transmission system namely gimbal drive which relocates motors from links to robot's base which results in suppression of motors weight in robot dynamic. In [5], an articulated robot is optimized in a way that maximum weight loss is achieved. Design of anti-backlash gear trains for precision positioning control systems has been studied in [6]. Reference [7] presented effects of harmonic drives elasticity in vibration of SCARA robots. Different adaptive controllers were tested on a direct drive SCARA robot and results of their performance were compared [8].

Kinematics and dynamics of SCARA robots were also derived and simulated using various software [9],[10]. In [9] experimental results of Serpent 1 were compared with simulations. Specific SCARA robots, five bar parallel SCARA and redundant joint SCARA have been studied in [11]-[13]. Additionally, different educational robots were constructed and controlled with PID [14],[15]. Finally mechanical design process of a novel star spherical parallel robot was illustrated in [16]. However, to the best of authors knowledge, no studies are available on the design of an industrial SCARA robot. In this paper, design process of a fast and accurate SCARA robot, comparable with its commercial countertype, is proposed.

II. FUM SCARA ROBOT DESIGN GOALS

The aim of designing this robot is to make an educational manipulator with characteristics similar to the world's leading commercial industrial robots. So, innovative control algorithms could be designed and implemented.

Design parameters of the robot include payload, reach and workspace, max velocity, accuracy and repeatability, arm stiffness and cost [17]. A mid-range size is considered for FUM SCARA to perform different tasks. Table I highlights characteristics of FUM SCARA in comparison with other industrial robots.

Fig. 1. FUM SCARA Robot

978-1-4799-6743-8/14/$31.00 ©2014 IEEE

TABLE I.
COMPARISON OF FUM SCARA VS. WELL KNOWN SCARA BRANDS

Specification	Units	**FUM SCARA**	Epson LS6	Yamaha YK700XG	Adept Cobra s800
Reach	mm	**700**	600	700	800
Linear Velocity	J1+J2 (mm/s)	**8500**	6800	8400	-
	J3/(mm/s)	**1100**	1100	2300	1100
	J4(°/s)	**1100**	2000	1020	1200
Repeatability	x,y (mm)	**±0.013**	±0.02	±0.02	±0.017
	z (mm)	**±0.023**	±0.01	±0.01	±0.003
	α (°)	**±0.016**	±0.01	±0.005	±0.019
Payload	(kg)	**6**	6	20	5.5

III. FUM SCARA KINEMATICS

Determining Denavit-Hartenberg parameters is the first step to derive robot's kinematics. The coordinate systems are attached to the robot according to DH convention and shown in Fig. 2. The established DH table of FUM SCARA is shown in table III. Using this table, kinematics of the robot will be obtained [18].

The relationship between 3rd motor and the prismatic joint is illustrated in (1).

$$d_4\,(m) = \frac{L}{2\pi}\theta_4\,(rad) \quad (1)$$

Direct kinematic is solved by multiplying transformation matrices shown in (2). By equating (3) and (4), and solving the equations for x, y, z and γ equation (5) is obtained.

$${}^0_5T = {}^0_1T\,{}^1_2T\,{}^2_3T\,{}^3_4T\,{}^4_5T \quad (2)$$

$${}^0_5T = \begin{bmatrix} c_{123} & s_{123} & 0 & l_1c_1 + l_2c_{12} \\ s_{123} & -c_{123} & 0 & l_1s_1 + l_2s_{12} \\ 0 & 0 & -1 & d_1 - d_5 - \dfrac{0.016}{2\pi}\theta_4 \\ 0 & 0 & 0 & 1 \end{bmatrix} \quad (3)$$

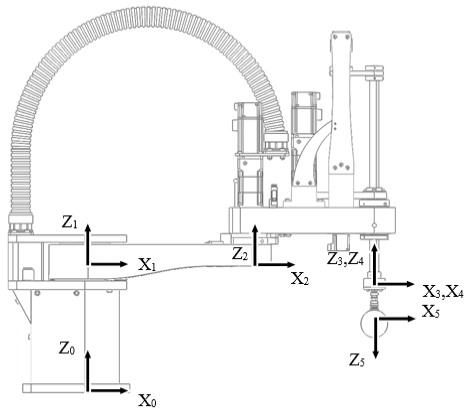

Fig. 2. Attached coordinate systems to SCARA robot

TABLE II. NOMENCLATURE

Symbol	Unit	Definition
α_{i-1}	*rad*	Angle from z_{i-1} to z_i measured along x_{i-1}
a_{i-1}	*m*	Distance from z_{i-1} to z_i measured along x_{i-1}
d_i	*m*	Distance from x_{i-1} to x_i measured along z_i
θ_i	*rad*	Angle from x_{i-1} to x_i measured along z_i
l_i	*m*	Link length
L	*m*	Lead of ball screw
${}^i_jT$	_	Transformation matrix, defines frame $\{j\}$ relative to $\{i\}$
c_1	_	$\cos(\theta_1)$
s_1	_	$\sin(\theta_1)$
c_{12}	_	$\cos(\theta_1+\theta_2)$
s_{12}	_	$\sin(\theta_1+\theta_2)$
c_{123}	_	$\cos(\theta_1+\theta_2+\theta_3)$
s_{123}	_	$\sin(\theta_1+\theta_2+\theta_3)$
x	*m*	x component of end effector position vector relative to base frame
y	*m*	y component of end effector position vector relative to base frame
z	*m*	z component of end effector position vector relative to base frame
γ	*rad*	Rotation of end effector relative to base frame
J	_	Jacobian matrix
v	*m / s*	Velocities in Cartesian coordinate system relative to base frame

TABLE III. FUM SCARA DENAVIT-HARTENBERG TABLE

i	α_{i-1} (rad)	a_{i-1} (m)	d_i (m)	θ_i (rad)
1	0	0	$d_1 = 0.295$	θ_1
2	0	$l_1 = 0.4$	0	θ_2
3	0	$l_2 = 0.3$	0	θ_3
4	0	0	d_4	0
5	π	0	$d_5 = 0.057$	0

$${}^B_WT = \begin{bmatrix} c_\gamma & s_\gamma & 0 & x \\ s_\gamma & -c_\gamma & 0 & y \\ 0 & 0 & -1 & z \\ 0 & 0 & 0 & 1 \end{bmatrix} \quad (4)$$

$$\begin{bmatrix} x \\ y \\ z \\ \gamma \end{bmatrix} = \begin{bmatrix} l_1\,c_1 + l_2c_{12} \\ l_1s_1 + l_2s_{12} \\ d_1 - d_5 - \dfrac{L}{2\pi}\theta_4 \\ \theta_1+\theta_2+\theta_3 \end{bmatrix} \quad (5)$$

Inverse kinematic of the robot is derived by solving (5). Four closed loop expressions are obtained for θ_i.

The relationship between Cartesian and joint space speed is derived by Jacobian as shown in (6).

TABLE IV. CONCEPT DESIGNS OF 2ND JOINT

Important Factors	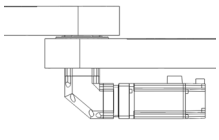	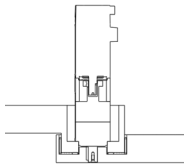	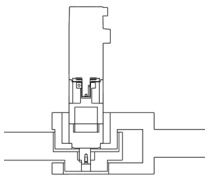	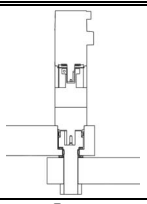
Joint Weight	High	Low	High	Low
Link Stiffness	High	Low	Moderate	High
Joint Range	Unlimited	Unlimited	Limited	Unlimited
Moment Acting on Gearbox Shaft	No	No	No	No
2nd Link Rotation Direction Relative to Motor Shaft	Same	Reverse	Same	Reverse

$$v = J(\theta)\dot{\theta} \quad (6)$$

Jacobian matrix of FUM SCARA is expressed in (7).

$$J(\theta) = \begin{bmatrix} -l_1 s_1 - l_2 s_{12} & -l_2 s_{12} & 0 & 0 \\ l_1 c_1 + l_2 c_{12} & 0 & 0 & 0 \\ 0 & 0 & 0 & -\dfrac{L}{2\pi} \\ 1 & 1 & 1 & 0 \end{bmatrix} \quad (7)$$

IV. MECHANICAL DESIGN

A. Transmission Selection

The mechanical design starts from initial concept to the final model. The initial concept of robot included links with estimated length, weight of equipment considering link density, power transmission system, and other probable components. Based on this data initial model of robot was prepared. Next, a trajectory is designed which is utilized for further simulations in a way that robot reaches its high speed and accelerations. Based on actual dynamic simulation results, motor and gearbox will be selected for each joint and subsequently their weight and inertia was modified in the model. This procedure was repeated until results of simulations met the selected transmission's power and speed. Fig. 3 shows the method of determining transmission system.

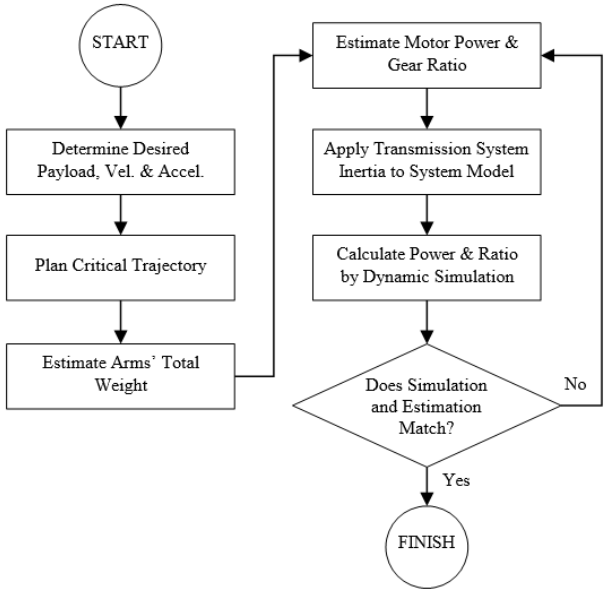

Fig. 3. Optimizing procedure of motor and gearbox selection

B. Joints Design

Design of robot joints started after power transmission system was determined. In the joint design process, additional details were considered such as assemblability, machinability and existence of dimensionally suitable bearings. Simultaneously, to acquire the largest possible workspace, mechanical components should not interfere with joint ranges.

1) First Joint

In order to prevent exertion of bending moments on gearbox shaft resulting from arms' weight, structure of robot base supports first link from two sides. In this joint to eliminate any additional backlash, motor torque transmits to the link by a power lock, instead of traditional methods.

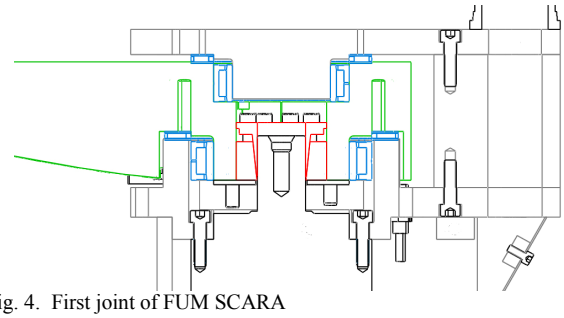

Fig. 4. First joint of FUM SCARA

Fig.4 demonstrates all the components used in this joint.

2) Second Joint

A basic principle in robot's design was the capability of assembling robot without using motors and gearboxes as a part of robot mechanism. Because of this principle, in all designs of 2nd joint a custom coupling is used in order to prevent effects of bending moments on gearbox shaft. Advantages of second joint's different concept designs are compared in table IV.

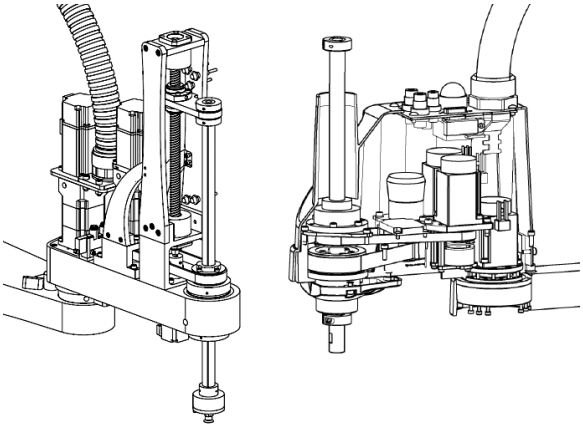

Fig. 5. FUM SCARA (on the left) uses a custom combination of ball bearing and ball spline while Epson LS SCARA (on the right) benefits from special ordered ball screw/spline.

3) Revolute Prismatic Joint

The third and fourth joints which allows robot end effector linear and rotational movement respectively, are created by coupling a ball screw to a ball spline. Using simple ball spline instead of a more expensive traditional rotary ball spline, reduced joint size due to use of compact needle bearings as well as reduction in design cost. This design made the overall design more complicated and of course less expensive. Fig. 5 demonstrates difference of 3rd and 4th joints in FUM SCARA and Epson LS SCARA robot.

V. Defining Dynamic Simulations' Test Path

To simulate the robot dynamic, Matlab software was used and a critical path, namely test trajectory was created. The test trajectory consists of a path which initially places the robot at one end of its joint range so that 1st and 2nd links are located (positioned) at the corner of the workspace. Next, it requires the robot to move to its other corner. The robot reaches its highest speed in the middle of the path. Please see Fig. 6. The features of the path are as follows:

- Both 1st and 2nd joints simultaneously reach the specified maximum velocity
- When two links become collinear –in the middle of the path- highest velocity is achieved. Since in this position links' center of gravity keeps the farthest distance to the base, the lateral forces will become their maximum value
- The rotational acceleration becomes maximum when links are collinear

Trajectory is created in joint space using a 7th degree polynomials.

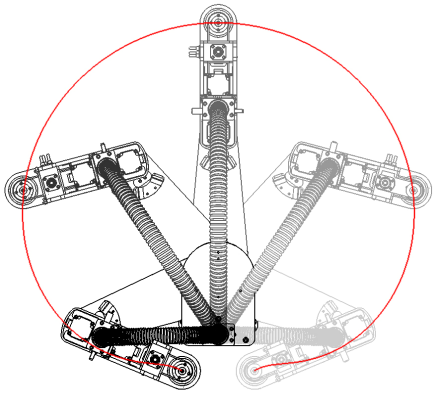

Fig. 6. Test Trajectory – Trajectory starts from one corner of workspace (light gray) to the opposite side (black). The path traced by end effector is shown.

VI. Workspace

Location of sensors, mechanical stops and design of components are designed in a way to allow the robot for its maximum joint ranges and a relatively larger workspace. Joint ranges are shown in table V.

FUM SCARA has a relatively large dexterous workspace where the work piece could be oriented in any direction about z axis.

VII. Experimental Results

Using a PID controller, performance of robot was tested in the test trajectory. Fig. 8 demonstrates the accuracy of the robot's position and speed as when compared with a desired

TABLE V. Robot Workspace

Joints	Work Envelope
J1	±110deg
J2	±130deg
J3	190mm
J4	∞

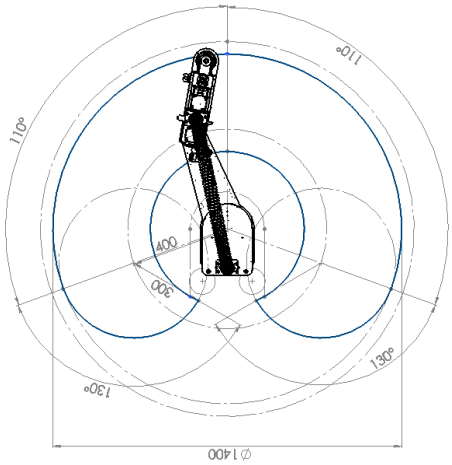

Fig. 7. FUM SCARA Workspace

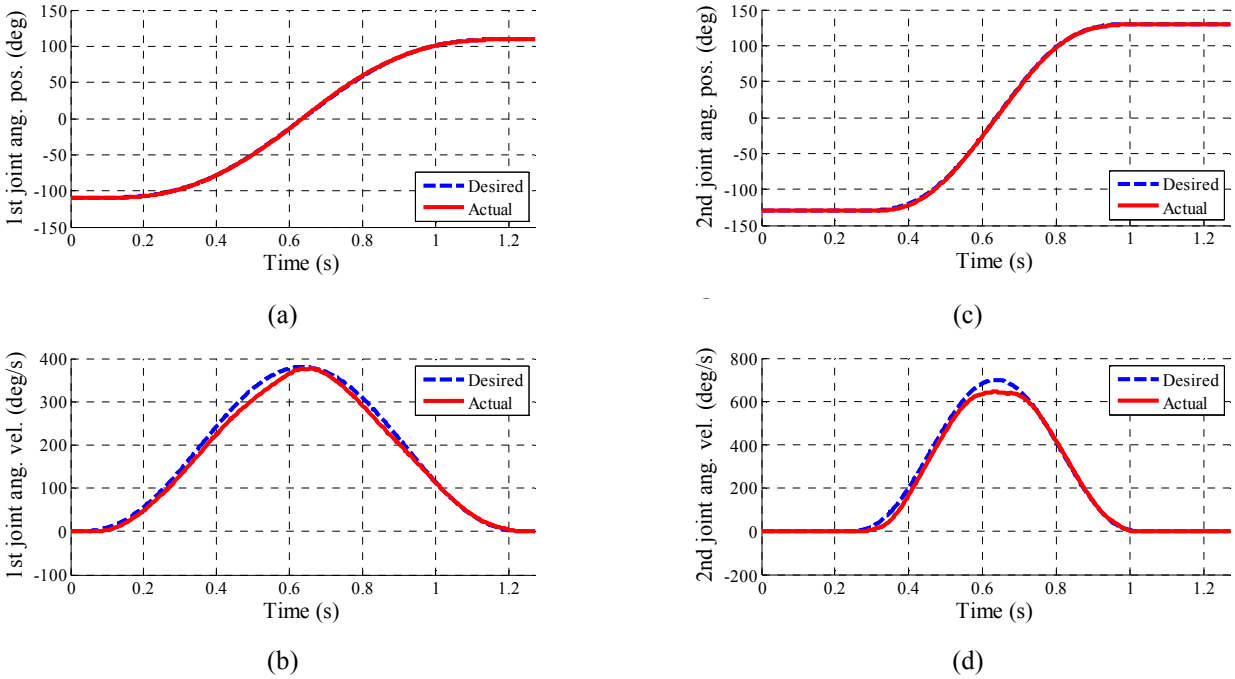

Fig. 8. Performance of FUM SCARA in test trajectory with PID controller: (a) and (b) demonstrates first joint angular position and velocity, (c) and (d) demonstrates second joint angular position and velocity, respectively.

trajectory. In these figures desired output is shown with continuous line and actual output is shown with dashed line. As shown, the two trajectories follow each other quite nicely which demonstrates the ability of the robot to follow a desired trajectory.

VIII. Conclusion

In this paper, some of the steps taken in design process of the FUM SCARA robot were illustrated. A special test trajectory, in which the robot reaches its maximum speed, was designed. End effector of the FUM SCARA robot was able to reach speeds as high as 8.5 m/sec, with repeatability of 0.013mm, 0.005mm, 0.023mm and 0.016deg for its x,y,z and α axis, respectively. Experimental results of robot motion using a conventional PID controller and the test trajectory were compared with simulations. It is shown that the test trajectory is followed with great accuracy in position and speed. Finite element analysis was used to minimize the total weight of the robot links. Use of planetary gearboxes instead of harmonic drives presented significantly more challenges by requiring use of a customized bearing assembly, increasing overall joint design as well as increasing the link weight and inertia. Additionally, their selection resulted in having to use larger motors with higher powers. However, these drives better met the project cost goals and were readily available in Iran. Finally, in addition to having industrial capability, the use of open architecture in its control system, enables this robot to be used as a great research tool. The authors believe that, the FUM SCARA is among the most economical SCARA robots with unique and competing industrial specifications.

References

[1] L. Westerlund, *The Extended Arm of Man: A History of Industrial Robot*: Informationsförlaget, 2000.

[2] S. Y. Nof, *Handbook of Industrial Robotics*: Wiley, 1999.

[3] K.-S. Hong, K.-H. Choi, J.-G. Kim *et al.*, "A PC-based open robot control system: PC-ORC," *Robotics and Computer-Integrated Manufacturing,* vol. 17, no. 4, pp. 355-365, 2001.

[4] P. Turner, P. Nigrowsky, and G. Vines, "A new approach for the design of robot joint transmission," *Mechatronics,* vol. 11, no. 8, pp. 1053-1062, 2001.

[5] L. Zhou, S. Bai, and M. R. Hansen, "Design optimization on the drive train of a light-weight robotic arm," *Mechatronics,* vol. 21, no. 3, pp. 560-569, 2011.

[6] L. C. Hale, and A. H. Slocum, "Design of anti-backlash transmissions for precision position control systems," *Precision engineering,* vol. 16, no. 4, pp. 244-258, 1994.

[7] G. Legnani, and R. Faglia, "Harmonic drive transmissions: the effects of their elasticity, clearance and irregularity on the dynamic behaviour of an actual SCARA robot," *Robotica,* vol. 10, no. 4, pp. 369-375, 1992.

[8] M. K. Cılız, and M. O. Tuncay, "Comparative experiments with a multiple model based adaptive controller for a SCARA type direct drive manipulator," *Robotica,* vol. 23, pp. 721-729, 2005

[9] M. T. Das, and L. Canan Dülger, "Mathematical modelling, simulation and experimental verification of a scara robot," *Simulation Modelling Practice and Theory,* vol. 13, no. 3, pp. 257-271, 2005.

[10] M. S. Alshamasin, F. Ionescu, and R. T. Al-Kasasbeh, "Kinematic modeling and simulation of a SCARA robot by using solid dynamics and verification by matlab/simulink," *European Journal of Scientific Research, ISSN*, pp. 388-405, 2009.

[11] L. Campos, F. Bourbonnais, I. A. Bonev *et al.*, "Development of a five-bar parallel robot with large workspace." pp. 917-922.

[12] A. Burisch, S. Soetebier, J. Wrege *et al.*, "Design of a parallel hybrid micro-scara robot for high precision assembly." p. 1374.

[13] C. Urrea, and J. Kern, “Modeling, simulation and control of a redundant SCARA-type manipulator robot,” *International Journal of Advanced Robotic Systems,* vol. 9, 2012.
[14] K. S. Mohamed Sahari, K. H. Weng, Y. W. Han *et al.*, “Design and development of a 4–dof SCARA robot for educational purposes,” *Jurnal Teknologi,* vol. 54, no. 1, pp. 193–215, 2012.
[15] M. S. Dutra, and C. J. Diaz, “Design and construction of a manipulator type SCARA, implementing a control system,” 2007.
[16] N. Mahpeykar, J. Enferadi, and A. Akbarzadeh, "Mechanical design process for the zippy wrist." pp. 1-8.
[17] P. Bhatia, J. Thirunarayanan, and N. Dave, “An expert system-based design of SCARA robot,” *Expert Systems with Applications,* vol. 15, no. 1, pp. 99-109, 1998.
[18] J. Denavit, “A kinematic notation for lower-pair mechanisms based on matrices,” Trans. of the ASME. Journal of Applied Mechanics, vol. 22, pp. 215-221, 1955.